

13. SEDIMENTATION RATES OF THE SOUTHERN MEXICO CONTINENTAL MARGIN, DEEP SEA DRILLING PROJECT LEG 66¹

L. E. Shephard,² Department of Oceanography, Texas A&M University, College Station, Texas
and
Kenneth J. McMillen, Gulf Research and Development Company, Pittsburgh, Pennsylvania

INTRODUCTION

Sediment accumulation rates, computed using age-sediment thickness curves obtained from DSDP cores, are rarely corrected for compaction or bedding attitude to better approximate true sediment accumulation rates (c.f. van Andel et al., 1975; Davies et al., 1977; and Whitman and Davies, 1979). Variations with depth in either of these factors can hinder interpreting relative rates of sedimentary processes associated with a particular depositional environment. This problem becomes particularly relevant for convergent margin sediments, which often display variable bedding attitudes and pronounced changes in porosity, bulk density, and other parameters related to the compaction process at shallow depth. These rapid shallow changes render correlation of sedimentation rates within a single transect of holes very difficult. Two techniques have been applied to data collected from a transect of holes along the southwestern Mexico continental margin, DSDP Leg 66 (Fig. 1), to correct sediment accumulation rates for variations in compaction and bedding attitude. These corrections should help resolve true fluctuations in accumulation rates and their implications regarding convergent margin processes.

TECHNIQUES

Uncompacted sedimentation rates (m/m.y.) were computed utilizing porosity depth profiles and laboratory consolidation data in the following relationship to determine original sediment thickness, H_o :

$$H_o = H_p [(1 - n_p) \cdot (1 - n_o)^{-1}],$$

where H_p = thickness of present interval, n_p = *in situ* porosity of present interval, and n_o = porosity of sediment at time of deposition (Hamilton, 1959; 1976; Margara, 1968; and Behrens, 1980). Interval thicknesses varied from 10 to 50 meters depending on the rate of change in porosity with depth. In general, as the porosity gradient decreased with depth the interval thickness was increased. Porosity was determined gravimetrically on shipboard and in the laboratory, using an air comparison pycnometer. In addition, porosity was computed using average sediment grain densities for each site and water content values of sediment rock samples (Shephard et al., this volume). An approximated best fit line through the data from each site was used for determining present interval porosities at a particular depth (Fig. 2). *In situ* interval porosities were calculated using consolidation test results, in particular the rebound portion of the void ratio logarithm of pressure curve, to correct present interval porosities for volume changes resulting from the removal of overburden pressure (Fig. 3).

Hamilton (1976; pp. 286, and 296) presents a detailed discussion of the technique used for predicting *in situ* porosity values. Predicted values for changes in porosity due to removal of overburden pressure for Leg 66 data (% rebound in porosity) agree very well with those values determined by Hamilton for terrigenous sediments.

Mass sediment accumulation rates (gm/cm²/10³ years), also computed utilizing porosity and bulk density data to account for sediment volume changes, were derived using the relationship of van Andel et al. (1975):

$$R = (\gamma\beta - 0.01025 n_p) (A \times 10^{-1}),$$

where R = mass sediment accumulation rate (gm/cm²/10³ years), $\gamma\beta$ = bulk density (gm/cm³), n_p = sediment porosity, and A = modified age versus depth rate (m/10⁶ years).

The following assumptions underlay the computation of both uncompacted sedimentation rates and mass sediment accumulation rates: (1) the lithologic section is uniform; (2) the Quaternary surficial sediment index properties are representative of the index properties for underlying, older sediments at the time of deposition; (3) volume change, hence variations in index properties, results only from dewatering and is not a result of cementation; and (4) the percentage of rebound computed from e -log P curves is representative of that occurring in nature as a result of the removal of overburden pressure. The first two assumptions are very reasonable, because geotechnical property analyses were limited to clayey silts and silty clays having similar lithologies. Cementation, resulting in lower porosity and high bulk density values, is probably a factor only in the lower Miocene sandstones at Sites 489 and 493. Compaction corrections for these sediments would result in sediment accumulation rates which are too great. Schmertmann (1955) found predicted rebound percentages using consolidation test data closely approximate that which occurs in nature because of overburden removal.

In addition to the foregoing assumptions, the standard age-sediment thickness curves were initially corrected for bedding attitudes averaged over intervals of consistent high, medium, or low dips (Lundberg, this volume). This correlation is approximate because the cores were not oriented with respect to dip prior to splitting and not all bedding attitudes are visible in the cores. No attempt has been made to account for faulting or slumping.

RESULTS

To facilitate comparisons and interpretations, mass sediment accumulation rates (Fig. 4) and uncompacted sedimentation rates (Figs. 5-10; Table 1) are discussed for each depositional environment; outer slope Site 487; inner slope Sites 488, 491, and 492; middle slope Site 490; and upper slope Sites 489 and 493. In addition, a trench mass sediment accumulation rate of 400 gm/cm²/10³ years has been estimated for comparative purposes using bulk-density measurements from piston cores obtained in the area and trench wedge thicknesses and inferred age based on convergence rates for a steady state model (Karig and Sharman, 1975).

Site 487 mass sediment accumulation rates ranged from 10 to 13 gm/cm²/10³ years in the upper 105 meters

¹ Initial Reports of the Deep Sea Drilling Project, Volume 66.

² Present address: Sandia National Laboratories, Division 4536, Albuquerque, New Mexico.

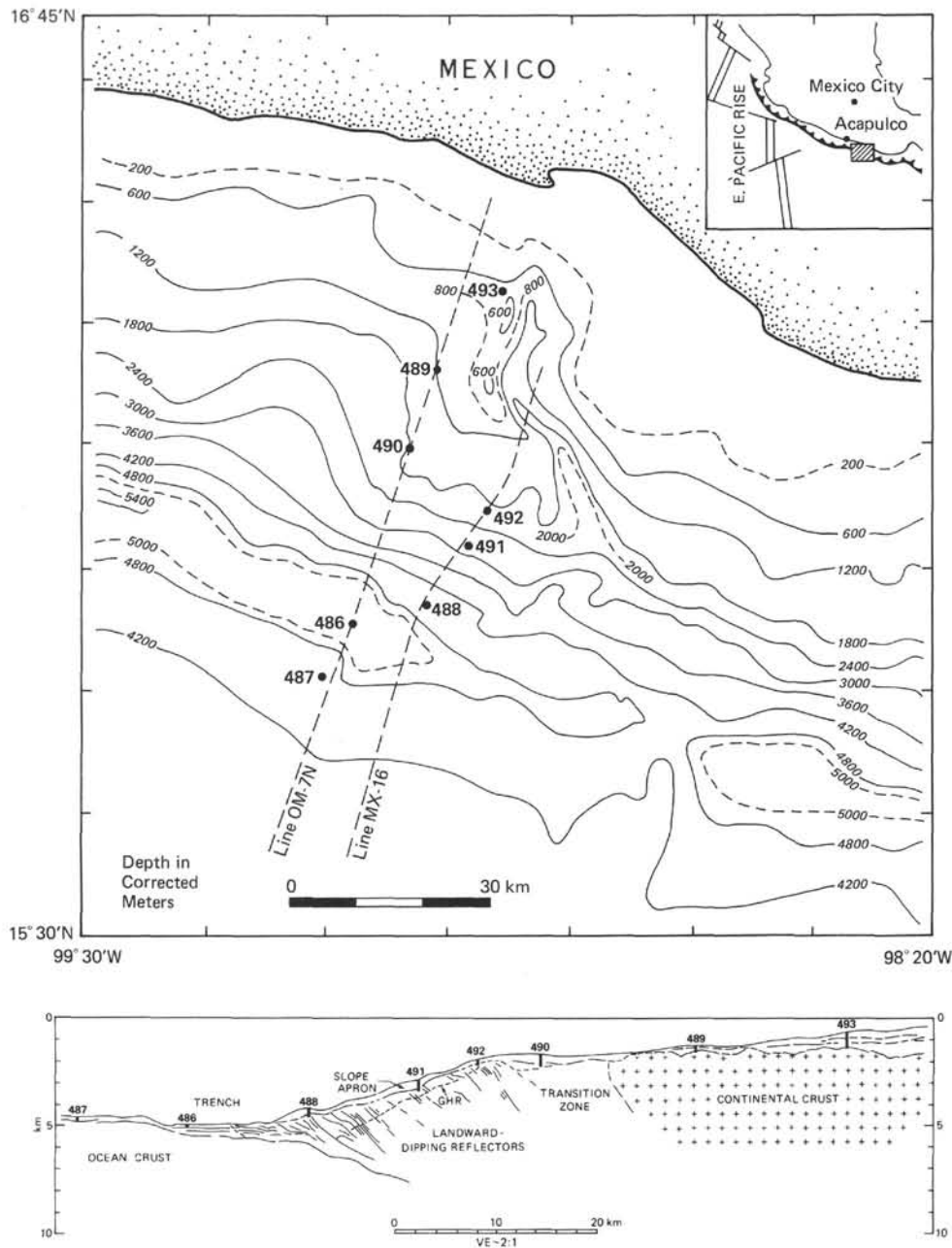


Figure 1. Location of Leg 66 drill sites along the southwestern Mexico continental margin. Schematic cross section represents a composite of multichannel seismic reflection profiles Lines OM-7N and MX-16.

of hemipelagic clayey silts below which pelagic red clays accumulated from 0.1 to 1.0 gm/cm²/10³ years. Because porosity showed little variation with depth, compacted and uncompact sedimentation rates were essentially equal, with values of 135 m/m.y. for the hemipelagic sediments and 3 to 30 m/m.y. for the pelagic red clays.

Lower inner trench slope Site 488 has fairly uniform mass sediment accumulation rates ranging from 32 to 49 gm/cm²/10³ years. Uncompact sedimentation rates are approximately double the compacted rates and vary from 490 to 620 m/m.y. Inner trench slope Sites 491 and 492 have very similar values in the upper 70 meters. Mass sediment accumulation rates range from 2 to 5

gm/cm²/10³ years, and uncompact sedimentation rates are less than 75 m/m.y. Below 70 meters, however, these rates change drastically at Site 491. Mass sediment accumulation rates rise to 404 gm/cm²/10³ years, and uncompact sedimentation rates in excess of 5000 m/m.y. are computed. Maximum mass sediment accumulation rates of only 6.0 gm/cm²/10³ years and uncompact sedimentation rates of less than 80 m/m.y. occur throughout the remainder of Site 492.

Middle slope Site 490, located between continental basement and the accretionary zone, has intermediate mass sediment accumulation rates of 10 to 45 gm/cm²/10³ years and high, variable uncompact sedimentation rates ranging from 42 to 609 m/m.y.

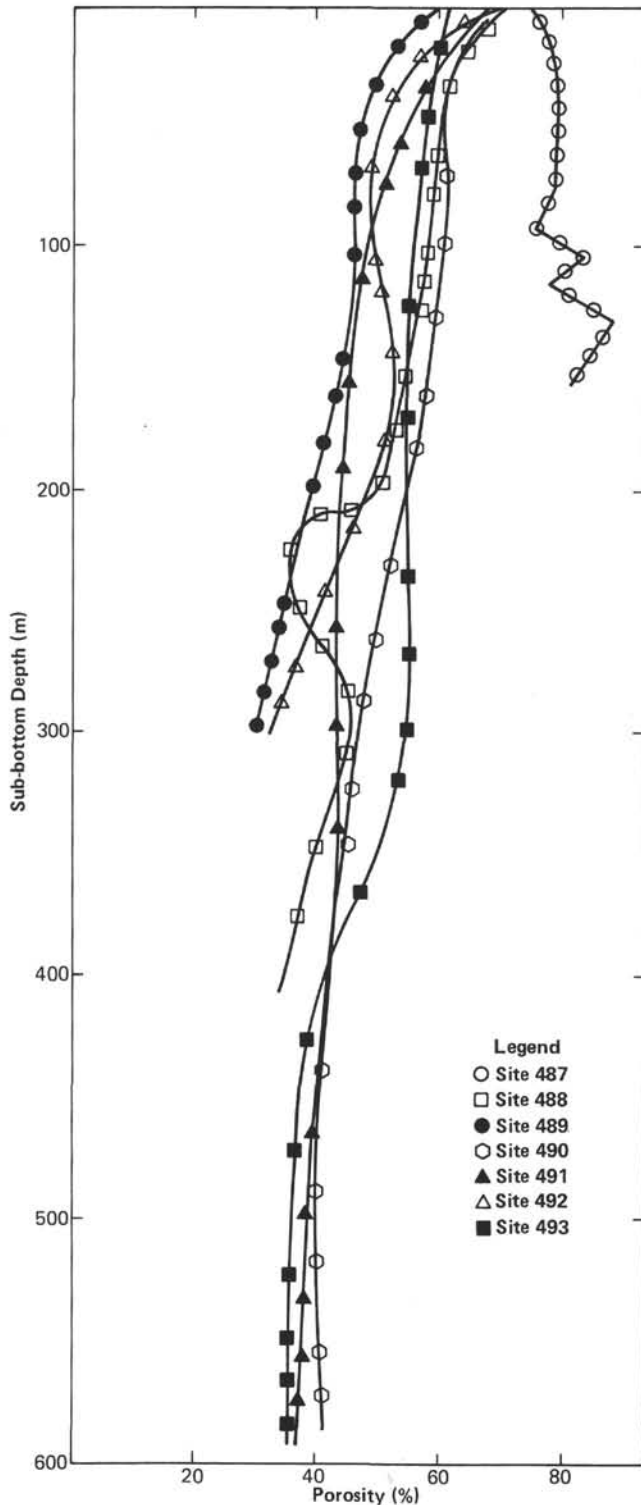


Figure 2. Interval porosity depth profiles used for computing *in situ* interval porosities to predict original sediment thicknesses.

Upper slope Site 489 has uniform mass sediment accumulation rates in the upper 140 meters ranging from 1.5 to 3 gm/cm²/10³ years and sedimentation rates less than 40 m/m.y. Below 140 meters mass sediment accumulation rates increase, ranging from 17 to 37 gm/cm²/10³ years, corresponding to an increase in uncom-

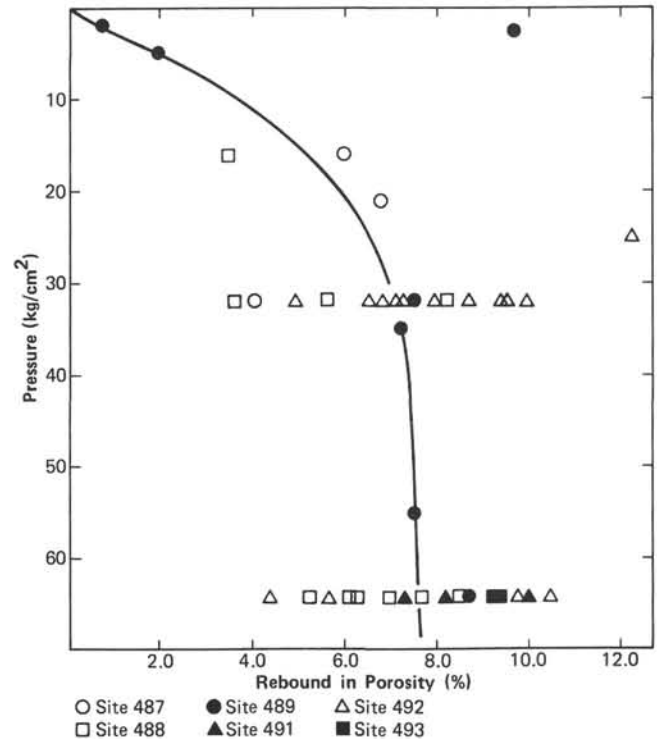


Figure 3. Amount of rebound in porosity resulting from unloading consolidation test samples performed on Leg 66 sediments. Interval porosities were corrected to *in situ* values by subtracting the correction factor for rebound in porosity, ϕ , determined using the following relationship: $\phi = 0.0599 + 0.4523P - 0.0091P^2 + 0.000016P^3$, where P (kg/cm²) is the effective overburden pressure calculated for the depth of the interval porosity used.

pacted sedimentation rates to 210 m/m.y. This change corresponds to a transgressive sequence overlying continental basement. Site 493 has fairly uniform mass sediment accumulation rates of 2.0 to 6.7 gm/cm²/10³ years and uncompacted sedimentation rates of less than 70 m/m.y. except for the lowermost section, which increases to 139 m/m.y.

DISCUSSION

Generalized convergent margin sedimentation models indicate that higher sediment accumulation rates occur in trench and lower slope environments whereas diminished rates occur in middle and upper slope environments. This variability results from sediment transport through submarine canyons bypassing upper and middle slope environments and resulting in greater lower slope and trench deposition (Underwood and Karig, 1980). Leg 66 Quaternary sediment accumulation rates from these environments illustrates the applicability of this model to the Middle America Trench region. Trench mass sediment accumulation rates estimated at 400 gm/cm²/10³ years are approximately an order of magnitude greater than lower inner slope rates at Site 488 (32–49 gm/cm²/10³). Quaternary rates for other inner, middle, and upper slope sediments range from 2 to 15 gm/cm²/10³ years. Site 488 uncompacted sedimentation rates vary less than 20%, indicating a uniform high

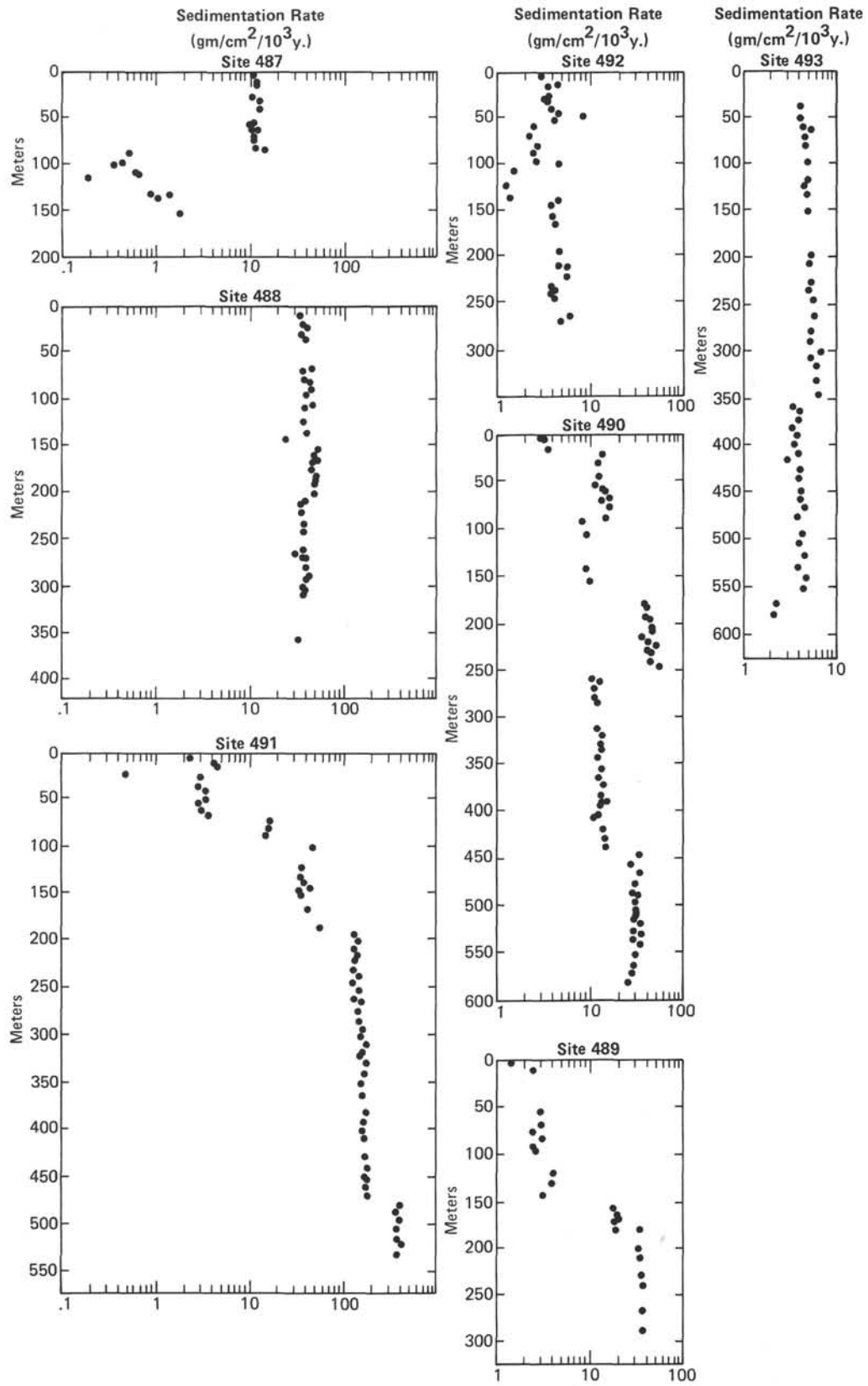


Figure 4. Mass sediment accumulation rates for Leg 66 sites. Rates for Middle America Trench Site 486 have been estimated from trench sediment thicknesses and a convergence rate of 10 cm/year, assuming that a steady-state trench model applies. Rates for the other sites were derived from initial sediment accumulation rates corrected for bedding dips and compaction.

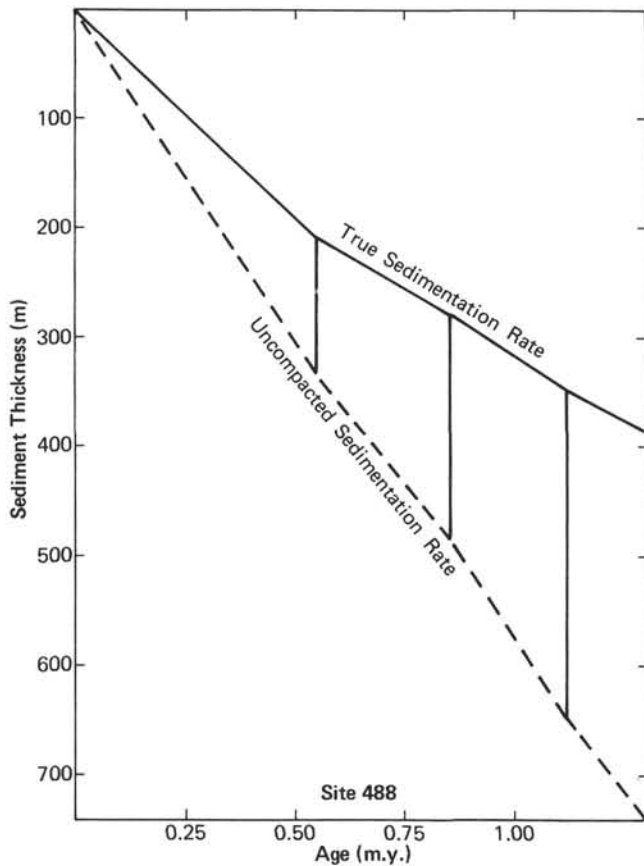


Figure 5. Sedimentation rate curves for Site 488 sediments. Routine age-sediment thickness relationships corrected for variations in bedding attitudes were used to determine the true sedimentation rate curve. Uncompacted sedimentation rate curve is corrected for variations in bedding attitude and compaction. (See Fig. 5 caption.)

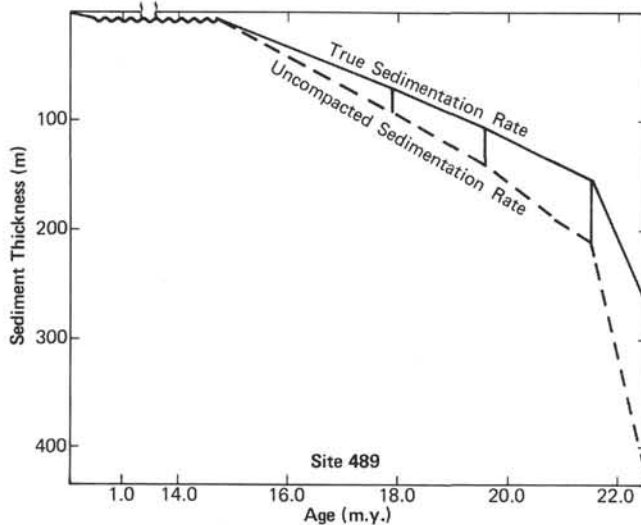


Figure 6. Sedimentation rate curves for Site 489 sediments. (See Fig. 5 caption.)

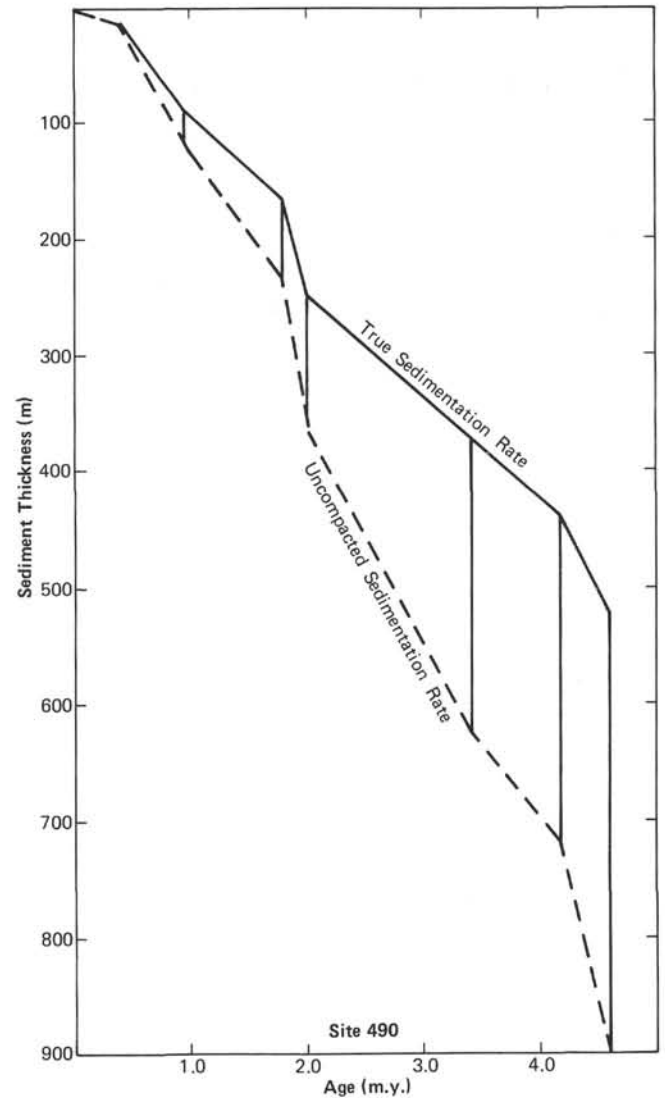


Figure 7. Sedimentation rate curves for Site 490 sediments. (See Fig. 5 caption.)

sediment influx into the lower slope area throughout the Quaternary. Outer slope hemipelagic sediments have accumulated at rates in excess of most upper and middle slope sites, $10 \text{ gm/cm}^2/10^3 \text{ years}$, resulting primarily from turbidite spillover from the trench. Outer slope brown pelagic clay accumulation rates, 0.1 to $1.0 \text{ gm/cm}^2/10^3 \text{ years}$, compare reasonably well with those established by Worsley and Davis (1979) for East Pacific pelagic sediment accumulation rates.

Site 491 mass sediment accumulation rates increase dramatically below 70 meters sub-bottom from less than 4 to over $400 \text{ gm/cm}^2/10^3 \text{ years}$. These values correspond to uncompacted sedimentation rates ranging from 7 m/m.y. to greater than 5000 m/m.y. toward the base of Hole 491. Lower Pliocene compacted sedimentation rates average greater than 800 m/m.y. , much higher than at any other site drilled. These exceptionally high sedimentation rates may result from deposition by mass movement processes or rapid, early Pliocene clayey silt deposition overlying sands within the trench or on the

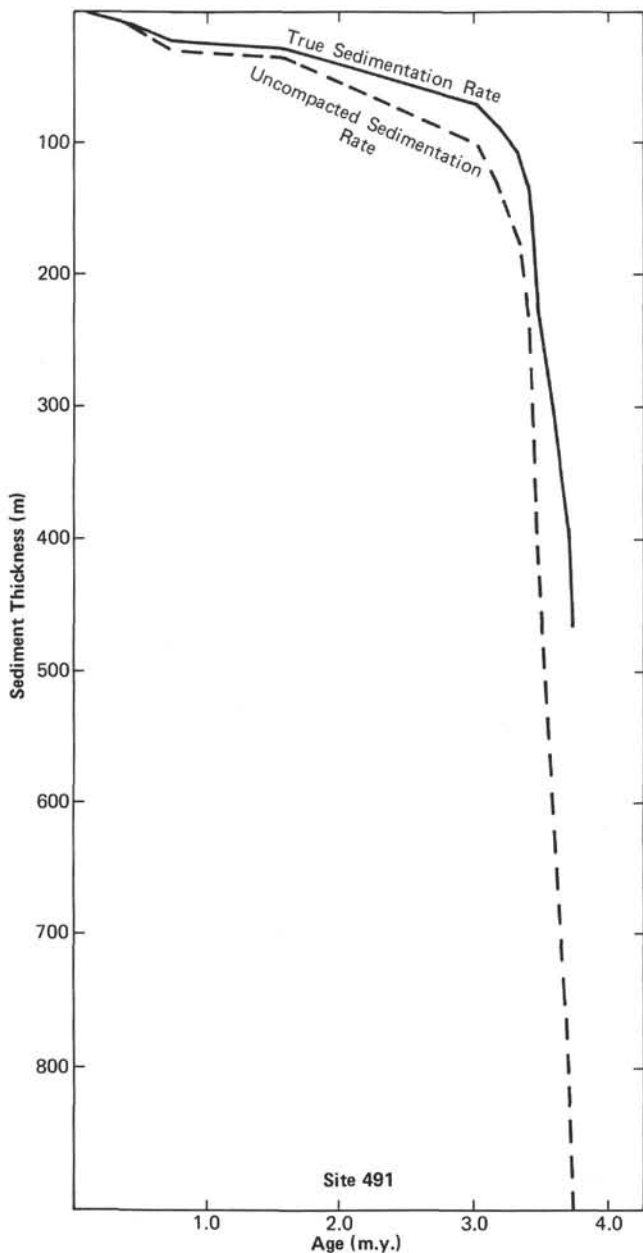


Figure 8. Sedimentation rate curves for Site 491 sediments. (See Fig. 5 caption.)

lower inner slope. Discontinuous and indistinct reflectors on seismic reflection profiles in the vicinity of Site 491 (see Shipley, this volume) are characteristic of sediment deposited by mass movement processes. Cored intervals within Lithologic Units 2 and 3 (see site Chapter) show variable dipping beds and apparent slump folds interpreted as synsedimentary deformation prior to tectonic deformation. Clayey silts toward the base of the hole immediately overlie lower slope or trench sands, indicating that initial deposition occurred within an area of high sediment accumulation rates as suggested by values reported for Sites 486 and 488.

Sediment accumulation rates of 2.3 to 6 gm/cm²/10³ year at Site 492 differ markedly from those at Site 491, remaining consistently low with depth to the sandy in-

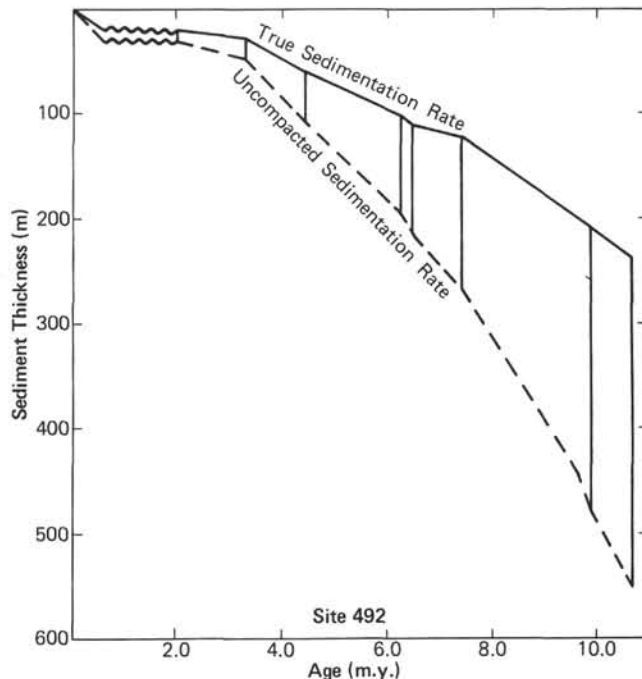


Figure 9. Sedimentation rate curves for Site 492 sediments. (See Fig. 5 caption.)

terval. These sands may represent uplifted trench sands at the base of the hole and suggest lower accumulation rates for the inner slope during the Miocene. Comparison of Pliocene mass sediment accumulation rates at Sites 490, 491, and 492 shows much higher values at Sites 490 and 491, indicating that Site 492 had been uplifted above Site 490 by this time, resulting in greater deposition landward of Site 492. Sediment bypassing and removal of sediment by slumping would also result in the lower Site 492 accumulation rates.

Previous convergent margin sedimentation rate analyses have been performed only for DSDP Leg 57, Japan Trench sediments (von Huene et al., 1978). These rates are generally lower than those of the Middle America Trench, averaging 2.5 gm/cm²/10³ years for the oceanic plate and 12.5 to 20 gm/cm²/10³ years for the lower trench inner slope. Middle trench slope accumulation rates of 10 to 15 gm/cm²/10³ years appear higher than those drilled in the Middle America Trench. A lack of sampling prevented determination of trench sediment accumulation rates offshore Japan. Differences in sediment accumulation rates between these margins are due to the decreased importance of sediment bypassing through submarine canyons off Japan, suggested by the similarities in lower and middle slope sedimentation rates, and the greater distance of the lower slope area from the shoreline.

CONCLUSIONS

Quaternary sedimentation rates for Leg 66 sediments indicate sediment bypassing of upper and middle slope environments through submarine canyons with subsequent deposition in lower inner slope and trench environments. Uniform sediment accumulation has oc-

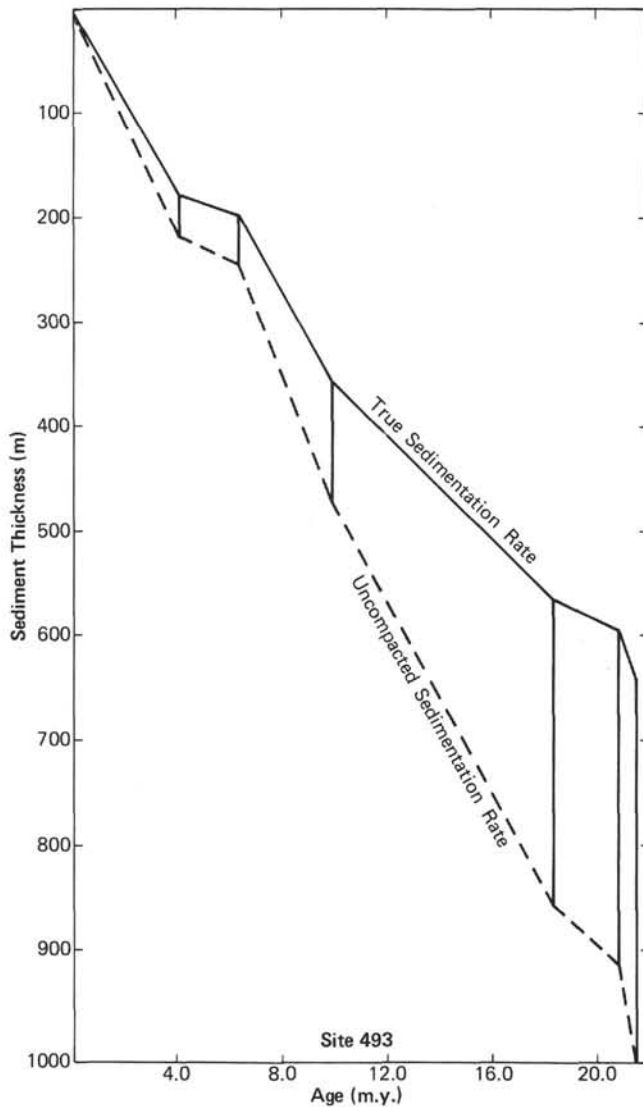


Figure 10. Sedimentation rate curves for Site 493 sediments. (See Fig. 5 caption.)

curred throughout the Quaternary within the lower slope environment, Site 488. Rapid sediment accumula-

tion rates increasing downhole in Site 491 are attributed to deposition by mass movement processes and initial deposition within the lower slope or trench areas. These areas represent the focus of deposition at margins where sediment transport occurs predominantly in submarine canyons. Low accumulation rates at Site 492 indicate uplift and subsequent sediment bypassing of this site with the possible removal of sediment by submarine processes.

Leg 66 mass sediment accumulation rates appear much higher than those computed for the Japan Trench lower slope and trench environments. Sediment bypassing appears more pervasive offshore Mexico and probably contributes to these higher rates.

ACKNOWLEDGMENTS

The manuscript was reviewed by W. R. Bryant and W. E. Hottman. Sandy Drews and Curtis Cohen provided technical assistance. Partial support was provided by the Circle Dillo Experiment Station, Snook, Texas.

REFERENCES

- Behrens, E. W., 1980. On sedimentation rates and porosity. *Mar. Geol.*, 35:M11-16.
- Davies, T. A., Hay, W. W., Southam, J. R., et al., 1977. Estimates of Cenozoic oceanic sedimentation rates. *Science*, 197:53-55.
- Hamilton, E. L., 1959. Thickness and consolidation of deep-sea sediments. *Geol. Soc. Am. Bull.*, 70:1399-1424.
- _____, 1976. Variations of density and porosity in deep-sea sediments. *J. Sediment. Petrol.*, 46:280-300.
- Karig, D. E., and Sharman, G. F., III, 1975. Subduction and accretion in trenches. *Geol. Soc. Am. Bull.*, 86:377-389.
- Magara, K., 1968. Compaction and migration of fluids in Miocene mudstone, Nagaoka Plain, Japan. *Bull. Am. Assoc. Pet. Geol.*, 52:2466-2501.
- Schmertmann, J. M., 1955. The undisturbed consolidation of clay. *Trans. Am. Soc. Civ. Eng.*, 120:1201-1233.
- Underwood, M. B., and Karig, D. E., 1980. Contrasting patterns of trench and trench-slope sedimentation. *Geology*, 8:432-436.
- van Andel, Tj. H., Heath, G. R., and Moore, T. C., 1975. Cenozoic history and paleoceanography of the central equatorial Pacific Ocean. *Geol. Soc. Am. Mem. 143*, Boulder, Colorado.
- von Huene, R., Nasu, N., et al., 1978. Japan Trench transected. *Geotimes*, 23:16-18.
- Whitman, J. M., and Davies, T. A., 1979. Cenozoic oceanic sedimentation rates: How good are they? *Mar. Geol.*, 30:269-284.
- Worsley, T. R., and Davis, T. A., 1979. Cenozoic sedimentation in the Pacific Ocean: Steps toward a quantitative evaluation. *J. Sediment. Petrol.*, 49:1131-1148.

Table 1. Uncompacted and compacted sedimentation rate values corrected for bedding attitudes. Sediment thickness drilled is the apparent thickness penetrated by drilling. True sediment thickness is corrected for bedding attitude.

Site	Sediment Thickness Drilled (m)	Uncompacted Sediment Thickness (m)	Age (m.y.)	True Sediment Thickness (m)	Uncompacted True Sediment Thickness	Approximate Bedding Attitudes	Sedimentation Rate (m/m.y.)	Uncompacted Sedimentation Rate (m/m.y.)	
488	0-210	0-335	0-0.55	210	335	0°	382	610	
	120-300	335-533	0.55-0.86	69	152	40°	222	490	
	300-380	533-720	0.86-1.12	69	162	30°	266	620	
	380-428	720-840	1.12-1.30	37	92	40°	206	510	
489	0-5	0-5	0-0.37	5	5	0°	13.50	13.5	
	5-70	5-91	14.60-17.90	65	86	0°	19.50	26	
	70-110	91-148	17.90-19.60	35	49	30°	20.50	29	
	110-160	148-222	19.60-20.80	32	48	50°	26.50	40	
	160-200	222-290	20.80-21.50	14	23	70°	18.50	33	
490	200-327	290-525	21.50-22.50	119	221	20°	120	221	
	0-15	0-17	0-0.40	15	17	10°	37.50	42	
	15-57	17-72	0.40-0.72	41	54	10°	128	168	
	57-94	72-121	0.72-0.95	35	48	10°	152	208	
	94-170	121-236	0.95-1.80	75	113	10°	88	133	
	170-253	236-376	1.80-2.03	82	138	10°	356.50	600	
	253-380	376-638	2.03-3.43	126	258	10°	90	184	
	380-480	638-879	3.43-4.18	64	91	50°	86.50	121	
	480-588	879-1119	4.18-4.60	83	184	40°	197.50	438	
	0-10	0-12	0-0.40	10	12	10°	25	30	
	10-24	12-30	0.40-0.71	14	18	10°	45	55	
	24-28	30-35	0.71-1.55	4	5	10°	5	6	
491	28-70	35-99	1.55-3.00	42	63	10°	29	43	
	70-90	99-131	3.00-3.15	19	32	10°	126.5	213	
	90-126	131-179	3.15-3.32	21	42	30°	123.5	247	
	126-162	179-245	3.32-3.38	31	57	30°	516.5	950	
	162-170	245-260	3.38-3.40	7	13	30°	350	650	
	170-280	260-495	3.40-3.46	78	166	45°	1300	2765	
	280-360	495-655	3.46-3.56	75	150	20°	750	1500	
	360-370	655-675	3.56-3.57	5	17	20°	500	1700	
	370-380	675-695	3.57-3.58	9	17	20°	900	1700	
	380-390	696-716	3.58-3.59	5	18	20°	500	1800	
	390-470	716-888	3.59-3.69	75	149	20°	750	1490	
	470-542	888-1050	3.69-3.72	71	160	10°	2366	5333	
	492	0-20	0-30	0-0.60	20	30	0°	33	50
		20-28	30-45	2.00-3.31	8	15	0°	6	11
		28-60	45-110	3.31-4.22	32	65	0°	35	71
		60-100	110-195	4.22-6.23	40	85	0°	20	42
		100-110	195-215	6.23-6.50	10	20	0°	37	74
110-140		215-280	6.50-7.40	10	50	40°	11	55	
140-230		280-475	7.40-9.58	79	169	30°	36	78	
230-250		475-530	9.58-9.94	10	48	30°	28	133	
250-279		530-609	9.94-10.65	24	68	30°	34	96	
493		0-180	0-220	0-4.14	177	217	10°	43	52
	180-200	220-247	4.14-6.50	18	25	20°	7.50	11	
	200-290	247-370	6.50-8.30	86	115	20°	43	64	
	290-365	370-485	8.30-9.87	75	115	0°	48	73	
	365-586	485-895	9.87-18.40	208	385	20°	24.50	45	
	586-617	895-955	18.40-20.80	29	56	20°	12.00	23	
	617-670	955-1058	20.80-21.50	50	97	20°	71.50	139	